

Supplementary material

March 1, 2012

Abstract

This supplementary material has five sections. The first shows the Snell's window height is not a factor in our design and can be chosen arbitrarily (if a lenslet is present, it must at least cover the lenslet). The second discusses, in terms of light-fields, the types of optics that allow distant scene convolution. The third shows an imaging example of Snell's window on our prototype. The fourth explains how our designs differ from previous work on optical filtering of planar scenes. The fifth discusses aperture thickness vignetting of a design's angular support.

1 Snell's window height

In the paper, we assumed the height of the Snell's window is exactly the image distance of the embedded lens. Here we show two derivations, one with this assumption and one without. Since the two equations we derive are equal, the height of the refractive material does not matter and we can set it to whatever value we choose.

1.1 Lenslet in a Snell's window as in the paper

In Figure 1 we show the setup as in the paper. Our approach is to derive an equation for the value of the exterior angle ω in terms of the exterior unrefracted angles in the design. We show this equation is identical in the next section, which is derived from the general case.

Consider the right angles containing θ'_1 , θ'_2 and θ' . The tangents of these angles are $\tan(\theta'_1) = \frac{x' + \frac{d}{2}}{v}$, $\tan(\theta'_2) = \frac{\|x' - \frac{d}{2}\|}{v}$ and $\tan(\theta') = \frac{v}{x'}$. They are related by the equation,

$$\frac{2}{\tan(\theta')} = \tan(\theta'_1) \pm \tan(\theta'_2) \quad (1)$$

where the sign choice depends on the sign of $(x' - \frac{d}{2})$. We substitute Snell's law relations $n_1 \sin(\theta'_1) = \sin(\theta_1)$ and $n_1 \sin(\theta'_2) = \sin(\theta_2)$, as well as $\theta_2 \mp \theta_1 = \omega$ to get,

$$\frac{2 \cos(\theta)}{\sqrt{n_1^2 - \cos^2 \theta}} = \frac{\sin(\theta_1 \pm \omega)}{\sqrt{(n_1)^2 - \sin^2(\theta_1 \pm \omega)}} \pm \frac{\sin(\theta_1)}{\sqrt{(n_1)^2 - \sin^2(\theta_1)}} \quad (2)$$

which is an expression for ω in terms of the exterior, unrefracted angles θ_1 and θ .

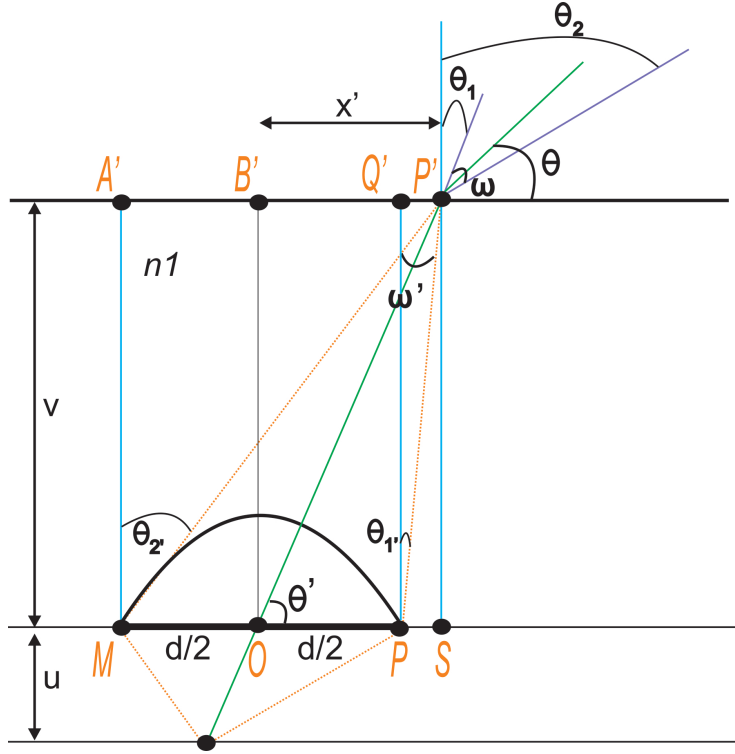


Figure 1: Lenslet in a Snell's Window (as in the paper)

1.2 General Lenslet in a Snell's window

In Figure 2 shows a lenslet placed in a refractive medium whose index of refractive is n_1 . The height of the refractive block is Z . Given this value as well as the viewing direction, θ and the angle of integration ω , we wish to find the corresponding values for the lenslet discussion in the paper, θ' and ω' .

From the $\triangle OO'B$, we can calculate the value of $Y = \frac{Z}{\tan(\theta')}$. Similarly we can get a relation for θ' , from the refraction at O' , since $\theta' = \frac{\pi}{2} - \arcsin \frac{\sin(\frac{\pi}{2} - \theta)}{n_1}$.

From $\triangle A'MM'$:

$$\tan(\theta_2') = \frac{\frac{d}{2} + Y + \frac{d'}{2}}{Z} \quad (3)$$

and from $\triangle PQ'P'$:

$$\tan(\theta_1') = \frac{Y - \frac{d}{2} - \frac{d'}{2}}{Z} \quad (4)$$

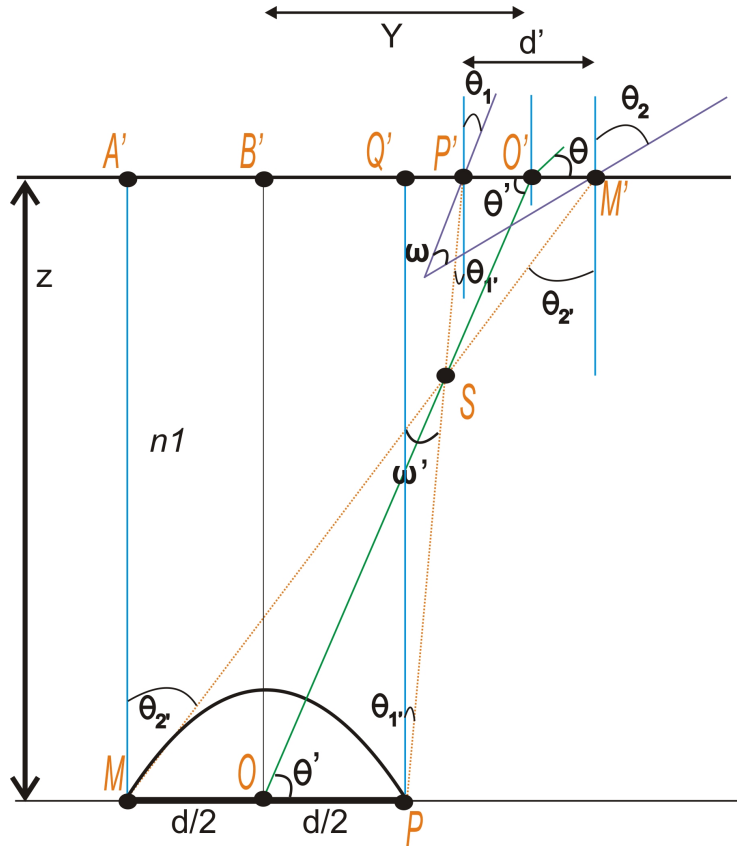


Figure 2: Lenslet in a Snell's Window (General Case)

Equating the $\frac{d'}{2}$ s (which are unknown):

$$\begin{aligned}
 Z \tan(\theta_{2'}) - \frac{d}{2} - Y &= Y - \frac{d}{2} - Z \tan(\theta_{1'}) \\
 2 * Y &= Z \tan(\theta_{2'}) + Z \tan(\theta_{1'}) \\
 \frac{2}{\tan(\theta')} &= \tan(\theta_{2'}) + \tan(\theta_{1'}) \\
 \frac{2}{\tan(\theta')} &= \frac{\sin(\theta_2)}{\sqrt{(n_1)^2 - \sin^2(\theta_2)}} + \frac{\sin(\theta_1)}{\sqrt{(n_1)^2 - \sin^2(\theta_1)}}
 \end{aligned}$$

Note that Z , the height of the slab, is out of the equation. This why, in our paper, we can assume Z to be a value that makes the calculation easier. In addition to the above equation, we have the the sum of angles for the triangle containing ω and the points P' and M' :

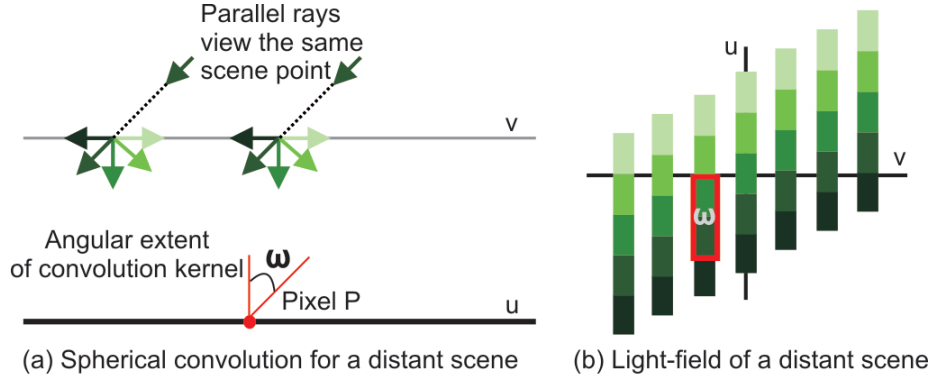


Figure 3: **Spherical convolution in terms of light-fields:** For a distant scene, spherical convolution on a planar sensor (a) integrates rays along a line curve in the light-field (b), suggesting quadratically curved optics [1], such as lenslets.

$$\begin{aligned}\omega + 90 + \theta_1 + 90 - \theta_2 &= 180 \\ \omega &= \theta_2 - \theta_1\end{aligned}$$

From the previous two equations, we can attempt to solve for θ_1 and θ_2 . From Snell's law and the solutions to these, we can obtain $\theta_{1'}$ and $\theta_{2'}$. Given these, from the vertex S of $\triangle SP'M'$, we get $\omega' = \theta_{2'} - \theta_{1'}$.

Now substituting $\sin(\theta_2) = \sin(\theta_1 + \omega)$, and from Snell's window, we get the exact two expressions as in the previous section:

$$\frac{2 \cos(\theta)}{\sqrt{n_1^2 - \cos^2 \theta}} = \frac{\sin(\theta_1 + \omega)}{\sqrt{(n_1)^2 - \sin^2(\theta_1 + \omega)}} + \frac{\sin(\theta_1)}{\sqrt{(n_1)^2 - \sin^2(\theta_1)}}$$

and

$$\frac{2 \cos(\theta)}{\sqrt{n_1^2 - \cos^2 \theta}} = \frac{\sin(\omega - \theta_1)}{\sqrt{(n_1)^2 - \sin^2(\omega - \theta_1)}} - \frac{\sin(\theta_1)}{\sqrt{(n_1)^2 - \sin^2(\theta_1)}}$$

2 The right optics for wide-angle filtering

Figure 3 (a) has a flatland light-field of a distant scene, similar to the light-field diagrams in [1]. In spherical convolution, we assign to sensor point P the light-rays covered by the solid angle ω marked as a linear region in Figure 3 (b). From [1]'s appendix, this suggests quadratically curved optics. At first glance, it would seem lenses should be sufficient for this purpose. However, the size of the linear region in the figure must be constant over different pixels, for correct spherical filtering. Unfortunately, in

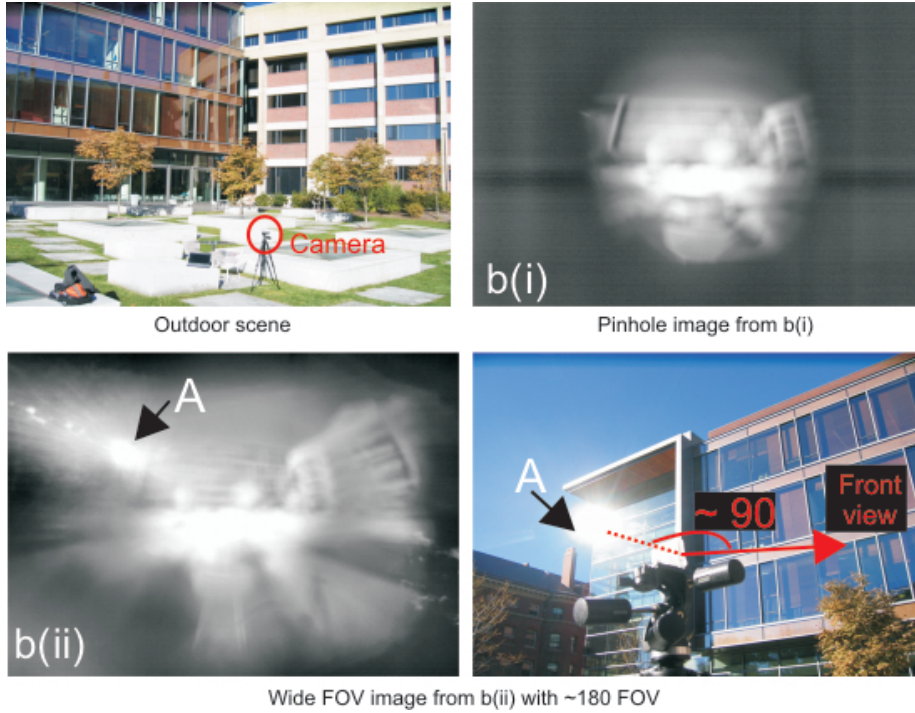


Figure 4: **Snell's window on outdoor scene:**

lenses, this region varies. In our CVPR 2011 paper, we have shown that a refractive slab comes close to approximating the correct filtering. In the future work section of our PAMI paper submission, we have shown a circular design for wide-angle filtering that has perfect spherical filtering.

3 An imaging example of Snell's window

In Fig. 4 we shown an imaging example of Snell's window (a miniaturized version of [2]) for an outdoor scene, showing that indeed our setup is able to provide 180 degree FOV and comparing it to a simple pinhole view of the same scene which has less FOV.

4 Lensless imaging for planar scenes vs. distant scenes

In Fig. 5 (left), $l_1 = l_2 = \|AB\| \frac{(v+u)}{u}$; the sensor convolves a stretched version of the template with a planar scene at a distance $(v+u)$. This is the scenario explained in [3]. However, for distant scenes defined on the hemisphere, the solid angle are important. $\triangle ABP_1$ and $\triangle ABP_2$ have the same base but different sides, and so the two angular supports are unequal; $\omega_1 \neq \omega_2$.

5 Aperture thickness vignetting:

In Fig. 5 (right), total occlusion occurs when $\arctan(\frac{t}{d}) = \arctan(\frac{u-t}{x-\frac{d}{2}})$. If $x < \frac{d}{2}$, no vignetting occurs. Elsewhere, the angular support decreases by $\omega_{vign} = \arccos(\frac{(y'+a)^2+(a')^2-(u-t)^2}{2(y'+a)(a')}}^{0.5}$, where $y' = ((\frac{t(x-\frac{d}{2})^2+u^2t^2}{u^2}))^{0.5}$, $a = (\frac{u^2(u-t)^2+((x-\frac{d}{2})u^2-t(x-\frac{d}{2}))^2}{u^2})^{0.5}$ and $a' = \frac{(4(u-t)^2+(2x-d)^2)^{0.5}}{2}$.

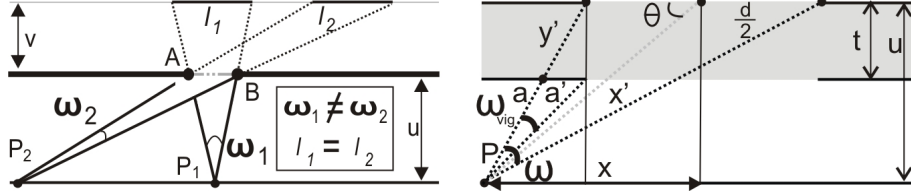


Figure 5: Lensless imaging and aperture vignetting

References

- [1] A. Levin, W. Freeman, and F. Durand. Understanding camera trade-offs through a bayesian analysis of light-field projections. *MIT CSAIL Tech. report 2008-049*, 2008. 4
- [2] R. W. Wood. Physical optics. *Macmillan*, 1911. 5
- [3] A. Zomet and S. Nayar. Lensless imaging with a controllable aperture. *CVPR*, 2006. 5